7th EUROMECH Solid Mechanics Conference
J. Ambrosio et.al. (eds.)
Lisbon, Portugal, 7–11 September 2009

AN EFFICIENT APPROXIMATION OF ORTHOTROPIC SET-VALUED FORCE LAWS OF NORMAL CONE TYPE

Michael Möller, Remco I. Leine and Christoph Glocker

Institute of Mechanical Systems, Center of Mechanics,
Department of Mechanical and Process Engineering,
ETH Zurich, CH-8092 Zurich, Switzerland
michael.moeller@imes.mavt.ethz.ch

Keywords: Non-Smooth Dynamics, Set-Valued Force Law, Normal Cone, Proximal Point, Ellipse, Coulomb-Contensou Friction.

Abstract. *The simulation of mechanical systems with set-valued friction laws requires the solution of normal cone inclusion problems. Orthotropic set-valued force laws can be approximated by inclusions using a normal cone on an elliptical set. In this paper, the transformation of normal cone inclusions and their corresponding proximal point equations is studied. The transformations lead to an efficient method for the solution of normal cone inclusions on elliptical sets. As an application, an approximated Coulomb-Contensou friction model is used in the numerical simulation of the Tippe-Top.*

1 INTRODUCTION

Non-smooth mechanical models with set-valued force laws of normal cone type are very useful for the analysis of the dynamics of mechanical systems with unilateral contacts and friction. Set-valued force laws for friction can not only describe the frictional interaction for sliding, but can also describe stiction. The formulation as normal cone inclusions provides a very general structure for a large class of force laws. For the numerical solution the normal cone inclusions are usually transformed to proximal point equations which are then iterated with a projected Jacobi or a projected Gauss-Seidel method. This requires a proximal point function to be available for each convex set used in the normal cone inclusions. Generally, the numerical evaluation of a proximal point function requires the numerical solution of an implicit function, which is numerically expensive. For one-dimensional sets, or simple multi-dimensional sets, this function can be formulated in explicit form yielding an efficient numerical evaluation and implementation. When confronted with a set with a more complex shape, one would like to transform the proximal point problem to a simpler set. One is tempted to try this transformation on the proximal point problem arising in the numerical implementation, because at this stage one usually gets aware of it, but this does not lead to a simplification. Nevertheless, it is possible to transform for example proximal point equations for elliptical sets to proximal point equations on circular sets. This can be achieved by transforming, at an earlier stage, directly the normal cone inclusion instead of the later proximal point problem, thereby exploiting the structure of the normal cone, and then deriving from the transformed normal cone inclusion the associated proximal point equation.

In section 2, an introduction to normal cones, proximal points and their relationships is given. The framework for the numerical simulation of non-smooth finite dimensional mechanical systems and the reduction to the core problem of solving a normal cone inclusion for every time step is described in section 3. The transformation of normal cone inclusions and their corresponding proximal point equations is discussed in section 4. The results from section 4 are then applied to the mechanical problem in section 5. Finally, the approximation and transformation of Coulomb-Contensou friction as well as the numerical results for the Tippe-Top are discussed in section 6.

2 NORMAL CONES AND PROXIMAL POINTS

The normal cone $\mathcal{N}_\mathcal{C}(\boldsymbol{x})$ to a convex set $\mathcal{C} \subset \mathbb{R}^n$ at the point $\boldsymbol{x} \in \mathcal{C}$ is the set of all vectors $\boldsymbol{y} \in \mathbb{R}^n$ which do not form an acute angle to any vector $\boldsymbol{x}^* - \boldsymbol{x}$ for all points $\boldsymbol{x}^* \in \mathcal{C}$, i.e.

$$\mathcal{N}_\mathcal{C}(\boldsymbol{x}) := \{\boldsymbol{y} \mid \boldsymbol{y}^\mathrm{T}(\boldsymbol{x}^* - \boldsymbol{x}) \leq 0,\ \forall \boldsymbol{x}^* \in \mathcal{C}\}. \tag{1}$$

If $\boldsymbol{x}$ is in the interior of $\mathcal{C}$, then the normal cone contains only the 0-element $\mathcal{N}_\mathcal{C}(\boldsymbol{x}) = \{0\}$. The normal cone is related to the problem of finding the proximal point to a convex set. For the definition of a proximal point a norm is required. With a symmetric and positive definite (PD) matrix $\boldsymbol{R} \in \mathbb{R}^{n\times n}$, the inner product of two vectors can be defined as

$$\langle \boldsymbol{x}, \boldsymbol{y} \rangle := \boldsymbol{x}^\mathrm{T}\boldsymbol{R}\,\boldsymbol{y}, \quad \boldsymbol{R} = \boldsymbol{R}^\mathrm{T},\ \boldsymbol{R}\,\mathrm{PD}. \tag{2}$$

This inner product naturally defines the norm $\|\boldsymbol{x}\|_R$ of a vector $\boldsymbol{x} \in \mathbb{R}^n$ as

$$\|\boldsymbol{x}\|_R = \sqrt{\langle \boldsymbol{x}, \boldsymbol{x} \rangle} = \sqrt{\boldsymbol{x}^\mathrm{T}\boldsymbol{R}\,\boldsymbol{x}}. \tag{3}$$

The proximal point $\operatorname{prox}_{\mathcal{C}}^{R}(\boldsymbol{x})$ of a point $\boldsymbol{x} \in \mathbb{R}^n$ to the convex set $\mathcal{C} \subset \mathbb{R}^n$ in the norm $\|.\|_R$ is the closest point in $\mathcal{C}$ to $\boldsymbol{x}$ with respect to the norm $\|.\|_R$,

$$\operatorname{prox}_{\mathcal{C}}^{R}(\boldsymbol{x}) := \underset{\boldsymbol{x}^* \in \mathcal{C}}{\operatorname{argmin}} \|\boldsymbol{x} - \boldsymbol{x}^*\|_R. \tag{4}$$

If $\boldsymbol{x}$ is in the set $\mathcal{C}$, then the proximal point $\operatorname{prox}_{\mathcal{C}}^{R}(\boldsymbol{x})$ is $\boldsymbol{x}$ itself. The proximal point function $\operatorname{prox}_{\mathcal{C}}^{R}$ is invariant to scaling of the matrix $\boldsymbol{R}$ of the associated norm $\|.\|_R$ by a positive scalar α,

$$\operatorname{prox}_{\mathcal{C}}^{R}(\boldsymbol{x}) = \operatorname{prox}_{\mathcal{C}}^{\alpha R}(\boldsymbol{x}), \quad \alpha \in \mathbb{R}^+. \tag{5}$$

The function $\operatorname{prox}_{\mathcal{C}}(\boldsymbol{x})$ denotes the proximal point function for the special case of the Euclidian norm which is obtained for $\boldsymbol{R} = \boldsymbol{I}$,

$$\operatorname{prox}_{\mathcal{C}}(\boldsymbol{x}) := \operatorname{prox}_{\mathcal{C}}^{I}(\boldsymbol{x}). \tag{6}$$

If a point $\boldsymbol{x}$ is the proximal point to the convex set $\mathcal{C}$ of the point $\boldsymbol{z}$, then the vector $\boldsymbol{z} - \boldsymbol{x}$ is an element of the normal cone $\mathcal{N}_{\mathcal{C}}(\boldsymbol{x})$. A normal cone inclusion can be reformulated equivalently as a proximal point problem,

$$\boldsymbol{z} - \boldsymbol{x} \in \mathcal{N}_{\mathcal{C}}(\boldsymbol{x}) \quad \Leftrightarrow \quad \boldsymbol{x} = \operatorname{prox}_{\mathcal{C}}(\boldsymbol{z}). \tag{7}$$

In the more general case where the proximal point function $\operatorname{prox}_{\mathcal{C}}^{R}(\boldsymbol{x})$ is used, this relationship becomes

$$\boldsymbol{y} \in \mathcal{N}_{\mathcal{C}}(\boldsymbol{x}) \quad \Leftrightarrow \quad \boldsymbol{x} = \operatorname{prox}_{\mathcal{C}}^{R}(\boldsymbol{x} + \boldsymbol{R}^{-1}\boldsymbol{y}). \tag{8}$$

To obtain this relationship, the proximal point function in the equation $\boldsymbol{x} = \operatorname{prox}_{\mathcal{C}}^{R}(\boldsymbol{x} + \boldsymbol{R}^{-1}\boldsymbol{y})$ is written as a minimization problem restricted to the convex set $\mathcal{C}$ by using the definition (4). Then, the restriction is replaced by adding the indicator function $\Psi_{\mathcal{C}}(\boldsymbol{x}^*)$ of the convex set $\mathcal{C}$ to the objective function of the minimization problem. If $\boldsymbol{x}$ is a point at which the minimum of $f(\boldsymbol{x}^*)$ is attained, then 0 has to be an element of the subdifferential ∂f. The subdifferential $\partial \Psi_{\mathcal{C}}(\boldsymbol{x})$ of the indicator function is just the normal cone $\mathcal{N}_{\mathcal{C}}(\boldsymbol{x})$ and one obtains the equivalent inclusion $\boldsymbol{y} \in \mathcal{N}_{\mathcal{C}}(\boldsymbol{x})$:

$$\begin{aligned}
&\boldsymbol{x} = \operatorname{prox}_{\mathcal{C}}^{R}(\boldsymbol{x} + \boldsymbol{R}^{-1}\boldsymbol{y}) \\
&\Leftrightarrow \boldsymbol{x} = \underset{x^* \in \mathcal{C}}{\operatorname{argmin}} \|\boldsymbol{x} + \boldsymbol{R}^{-1}\boldsymbol{y} - \boldsymbol{x}^*\|_R \\
&\Leftrightarrow \boldsymbol{x} = \underset{x^* \in \mathcal{C}}{\operatorname{argmin}} \frac{1}{2}\|\boldsymbol{x} + \boldsymbol{R}^{-1}\boldsymbol{y} - \boldsymbol{x}^*\|_R^2 \\
&\Leftrightarrow \boldsymbol{x} = \underset{x^*}{\operatorname{argmin}} \left(\frac{1}{2}\|\boldsymbol{x} + \boldsymbol{R}^{-1}\boldsymbol{y} - \boldsymbol{x}^*\|_R^2 + \Psi_{\mathcal{C}}(\boldsymbol{x}^*)\right) \\
&\Leftrightarrow \boldsymbol{x} = \underset{x^*}{\operatorname{argmin}} \left(\frac{1}{2}(\boldsymbol{x} - \boldsymbol{x}^*)^{\mathrm{T}}\boldsymbol{R}(\boldsymbol{x} - \boldsymbol{x}^*) + \boldsymbol{y}^{\mathrm{T}}(\boldsymbol{x} - \boldsymbol{x}^*) + \Psi_{\mathcal{C}}(\boldsymbol{x}^*)\right) \\
&\qquad f(\boldsymbol{x}^*) := \frac{1}{2}(\boldsymbol{x} - \boldsymbol{x}^*)^{\mathrm{T}}\boldsymbol{R}(\boldsymbol{x} - \boldsymbol{x}^*) + \boldsymbol{y}^{\mathrm{T}}(\boldsymbol{x} - \boldsymbol{x}^*) + \Psi_{\mathcal{C}}(\boldsymbol{x}^*) \\
&\Leftrightarrow \boldsymbol{x} = \underset{x^*}{\operatorname{argmin}} f(\boldsymbol{x}^*) \\
&\Leftrightarrow 0 \in \partial f(\boldsymbol{x}^*)\big|_{\boldsymbol{x}^* = \boldsymbol{x}} \\
&\Leftrightarrow 0 \in \big(-\boldsymbol{R}(\boldsymbol{x} - \boldsymbol{x}^*) - \boldsymbol{y} + \partial \Psi_{\mathcal{C}}(\boldsymbol{x}^*)\big)_{\boldsymbol{x}^* = \boldsymbol{x}} \\
&\Leftrightarrow 0 \in -\boldsymbol{y} + \partial \Psi_{\mathcal{C}}(\boldsymbol{x}) \\
&\Leftrightarrow \boldsymbol{y} \in \mathcal{N}_{\mathcal{C}}(\boldsymbol{x}).
\end{aligned} \tag{9}$$

Using this relationship, a normal cone inclusion can be formulated as a nonlinear equation, where the matrix $\boldsymbol{R}$ can still be chosen freely as long as it is symmetric and positive definite.

3 NON-SMOOTH DYNAMICS

The non-smooth dynamics of a finite-dimensional mechanical system is described by a differential inclusion for the impact-free motion and an impact inclusion which maps the left limit of the state to the right limit with respect to time. The generalized coordinates $\boldsymbol{q}(t) \in \mathbb{R}^f$ and the generalized velocities $\boldsymbol{u}(t) \in \mathbb{R}^k$ parameterize the state of the system. The right limit of $\boldsymbol{u}(t)$ is denoted by $\boldsymbol{u}^+$ and the left limit by $\boldsymbol{u}^-$. The generalized coordinates are continuous, meaning that their right and left limit $\boldsymbol{q}^+$ and $\boldsymbol{q}^-$ are identical. For this parameterization the differential inclusion for the impact-free motion becomes

$$\begin{aligned} \boldsymbol{M}(\boldsymbol{q},t)\dot{\boldsymbol{u}} - \boldsymbol{h}(\boldsymbol{q},\boldsymbol{u},t) - \sum_{i\in\mathcal{I}} \boldsymbol{W}_i(\boldsymbol{q},t)\boldsymbol{\lambda}_i = 0, \quad \dot{\boldsymbol{q}} = \boldsymbol{F}(\boldsymbol{q})\boldsymbol{u} \\ \boldsymbol{\gamma}_i = \boldsymbol{W}_i^{\mathrm{T}}(\boldsymbol{q},t)\boldsymbol{u} + \boldsymbol{\chi}_i(\boldsymbol{q},t), \quad \boldsymbol{\gamma}_i \in \mathcal{N}_{\mathcal{C}_i}(-\boldsymbol{\lambda}_i), \end{aligned} \tag{10}$$

and the impact inclusion has the form

$$\begin{aligned} \boldsymbol{M}(\boldsymbol{q},t)(\boldsymbol{u}^+ - \boldsymbol{u}^-) - \sum_{i\in\mathcal{I}} \boldsymbol{W}_i(\boldsymbol{q},t)\boldsymbol{\Lambda}_i = 0, \quad \boldsymbol{q}^+ - \boldsymbol{q}^- = 0 \\ \boldsymbol{\gamma}_i^{\pm} = \boldsymbol{W}_i^{\mathrm{T}}(\boldsymbol{q},t)\boldsymbol{u}^{\pm} + \boldsymbol{\chi}_i(\boldsymbol{q},t), \quad \boldsymbol{\gamma}_i^+ + \varepsilon_i\boldsymbol{\gamma}_i^- \in \mathcal{N}_{\mathcal{D}_i}(-\boldsymbol{\Lambda}_i). \end{aligned} \tag{11}$$

The matrix $\boldsymbol{M}(\boldsymbol{q},t) \in \mathbb{R}^{k\times k}$ is the symmetric and positive definite mass matrix and the vector $\boldsymbol{h}(\boldsymbol{q},\boldsymbol{u},t) \in \mathbb{R}^k$ contains all smooth forces. To transform the generalized velocities $\boldsymbol{u}$ to the derivative of the generalized coordinates $\dot{\boldsymbol{q}}$ the matrix $\boldsymbol{F}(\boldsymbol{q}) \in \mathbb{R}^{f\times k}$ is used. The set $\mathcal{I}$ contains all contacts i that are closed on displacement level. This can be expressed with the gap function $g_i(\boldsymbol{q},t)$ of every the contact

$$\mathcal{I} := \{i \mid g_i(\boldsymbol{q},t) = 0\}. \tag{12}$$

For every contact i there is a vector of relative velocities $\boldsymbol{\gamma}_i \in \mathbb{R}^{d_i}$, a vector of contact forces $\boldsymbol{\lambda}_i \in \mathbb{R}^{d_i}$ and a vector of contact percussions $\boldsymbol{\Lambda}_i \in \mathbb{R}^{d_i}$. The matrix $\boldsymbol{W}_i(\boldsymbol{q},t) \in \mathbb{R}^{k\times d_i}$ contains the generalized force directions of the contact. The set-valued force laws are formulated as normal cone inclusions $\boldsymbol{\gamma}_i \in \mathcal{N}_{\mathcal{C}_i}(-\boldsymbol{\lambda}_i)$ where the set $\mathcal{C}_i$ is the set of all admissible contact forces $\boldsymbol{\lambda}_i$. Newton's impact law in inclusion form with restitution coefficient ε_i is used, where the set $\mathcal{D}_i$ contains all admissible contact percussions $\boldsymbol{\Lambda}_i$.

For the numerical solution of (10) and (11) a time stepping scheme based on Moreau's midpoint rule [5] is used. Starting from a known state $\boldsymbol{u}^B = \boldsymbol{u}(t^B)$ and $\boldsymbol{q}^B = \boldsymbol{q}(t^B)$ at the time t^B of a time step Δt, the coordinates $\boldsymbol{q}^M = \boldsymbol{q}(t^M)$ at the midpoint are calculated

$$\boldsymbol{q}^M := \boldsymbol{q}^B + \frac{\Delta t}{2}\boldsymbol{F}(\boldsymbol{q}^B)\,\boldsymbol{u}^B, \quad t^M = t^B + \frac{\Delta t}{2} \tag{13}$$

Using the midpoint coordinates $\boldsymbol{q}^M$ and the velocities $\boldsymbol{u}^B$ from the beginning of the time step one calculates $\boldsymbol{M}(\boldsymbol{q}^M,t^M)$, $\boldsymbol{h}(\boldsymbol{q}^M,\boldsymbol{u}^B,t^M)$, $\boldsymbol{W}_i(\boldsymbol{q}^M,t^M)$, $\boldsymbol{\chi}_i(\boldsymbol{q}^M,t^M)$ and sets up the index set $\mathcal{I}$. As a next step one has to solve the inclusion

$$\begin{aligned} &\boldsymbol{M}(\boldsymbol{u}^E - \boldsymbol{u}^B) - \boldsymbol{h}\Delta t - \sum_{i\in\mathcal{I}} \boldsymbol{W}_i\boldsymbol{\Lambda}_i = 0, \\ &\boldsymbol{\gamma}_i^B = \boldsymbol{W}_i^{\mathrm{T}}\boldsymbol{u}^B + \boldsymbol{\chi}_i, \quad \boldsymbol{\gamma}_i^E = \boldsymbol{W}_i^{\mathrm{T}}\boldsymbol{u}^E + \boldsymbol{\chi}_i, \\ &\boldsymbol{\gamma}_i^E + \varepsilon_i\boldsymbol{\gamma}_i^B \in \mathcal{N}_{\mathcal{D}_i}(-\boldsymbol{\Lambda}_i), \end{aligned} \tag{14}$$

which approximates both the differential inclusion for the impact-free motion and the impact inclusion. As a result one obtains the end time velocities $\boldsymbol{u}^E$. Finally the end time coordinates have to be calculated

$$\boldsymbol{q}^E := \boldsymbol{q}^M + \frac{\Delta t}{2}\boldsymbol{F}(\boldsymbol{q}^M)\,\boldsymbol{u}^E, \quad t^E = t^M + \frac{\Delta t}{2}. \tag{15}$$

The core problem of an integration step is the solution of the inclusion (14). By introducing the abbreviations

$$\boldsymbol{\xi}_i := \boldsymbol{\gamma}_i^E + \varepsilon_i \boldsymbol{\gamma}_i^B, \quad \boldsymbol{G}_{ij} := \boldsymbol{W}_i^{\mathrm{T}} \boldsymbol{M}^{-1} \boldsymbol{W}_j, \quad \boldsymbol{c}_i := \boldsymbol{W}_i^{\mathrm{T}} \boldsymbol{M}^{-1} \boldsymbol{h} \Delta t + (1+\varepsilon_i)\boldsymbol{\gamma}_i^B \tag{16}$$

it can be rewritten as an inclusion problem of the form

$$\boldsymbol{\xi}_i \in \mathcal{N}_{\mathcal{D}_i}(-\boldsymbol{\Lambda}_i), \quad \boldsymbol{\xi}_i = \sum_j \boldsymbol{G}_{ij}\boldsymbol{\Lambda}_j + \boldsymbol{c}_i \tag{17}$$

which has to be solved for the discrete percussions $\boldsymbol{\Lambda}_i$. The end time velocities can then be calculated in an explicit way as

$$\boldsymbol{u}^E = \boldsymbol{u}^B + \boldsymbol{M}^{-1}\boldsymbol{h}\Delta t + \boldsymbol{M}^{-1}\sum_{i\,\in\,\mathcal{I}} \boldsymbol{W}_i \boldsymbol{\Lambda}_i. \tag{18}$$

The inclusion problem (17) consists of a normal cone inclusion and a linear equation for each set-valued force law. Further details on the non-smooth dynamics framework for mechanical systems that has been summarized in this section as well as advanced techniques can be found in [1, 6].

4 TRANSFORMATION OF NORMAL CONE INCLUSIONS

In this section the transformation of normal cone inclusions and proximal point problems under linear mappings of the underlying convex sets are discussed. For a convex set $\mathcal{C} \subseteq \mathbb{R}^n$ and a non-singular linear mapping $\boldsymbol{A} \in \mathbb{R}^{n\times n}$, $\det(\boldsymbol{A}) \neq 0$ the transformed set $\boldsymbol{A}\mathcal{C}$ consists of all the vectors $\boldsymbol{A}\boldsymbol{x}$ with $\boldsymbol{x} \in \mathcal{C}$. The inverse mapped set

$$\boldsymbol{A}^{-1}\mathcal{C} = \{\boldsymbol{y} \mid \boldsymbol{A}\boldsymbol{y} \in \mathcal{C}\} \tag{19}$$

contains all the vectors which are mapped by $\boldsymbol{A}$ to the set $\mathcal{C}$. The relationship between the normal cone to the set $\mathcal{C}$ and the normal cone to the set $\boldsymbol{A}^{-1}\mathcal{C}$ is given by

$$\mathcal{N}_{\mathcal{C}}(\boldsymbol{x}) = \boldsymbol{A}^{-\mathrm{T}}\mathcal{N}_{A^{-1}\mathcal{C}}(\boldsymbol{A}^{-1}\boldsymbol{x}), \tag{20}$$

for all $\boldsymbol{x} \in \mathcal{C}$. Of course, (20) can be written in the simpler form

$$\mathcal{N}_{\mathcal{C}}(\boldsymbol{x}) = \boldsymbol{A}^{\mathrm{T}}\mathcal{N}_{A\mathcal{C}}(\boldsymbol{A}\boldsymbol{x}), \tag{21}$$

but (20) is used in the following to keep all relations in this section between the set $\mathcal{C}$ and the inverse mapped set $\boldsymbol{A}^{-1}\mathcal{C}$. The relationship (20) can be obtained by injecting the identity matrix $\boldsymbol{I} = \boldsymbol{A}\boldsymbol{A}^{-1}$ into the definition of the normal cone (1) and manipulating the expression such

that one part transforms the argument and the set of the normal cone, and the other transforms the normal cone

$$\begin{aligned}\mathcal{N}_{\mathcal{C}}(\boldsymbol{x}) &= \{\boldsymbol{y} \mid \boldsymbol{y}^{\mathrm{T}}(\boldsymbol{x}^* - \boldsymbol{x}) \leq 0,\ \forall \boldsymbol{x}^* \in \mathcal{C}\} \\ &= \{\boldsymbol{y} \mid \underbrace{\boldsymbol{y}^{\mathrm{T}}\boldsymbol{A}}_{=:\,\boldsymbol{z}^{\mathrm{T}}}\boldsymbol{A}^{-1}(\boldsymbol{x}^* - \boldsymbol{x}) \leq 0,\ \forall \boldsymbol{x}^* \in \mathcal{C}\} \\ &= \{\boldsymbol{A}^{-\mathrm{T}}\boldsymbol{z} \mid \boldsymbol{z}^{\mathrm{T}}(\boldsymbol{A}^{-1}\boldsymbol{x}^* - \boldsymbol{A}^{-1}\boldsymbol{x}) \leq 0,\ \forall \boldsymbol{A}^{-1}\boldsymbol{x}^* \in \boldsymbol{A}^{-1}\mathcal{C}\} \\ &= \boldsymbol{A}^{-\mathrm{T}}\{\boldsymbol{z} \mid \boldsymbol{z}^{\mathrm{T}}(\boldsymbol{x}^\circ - \boldsymbol{A}^{-1}\boldsymbol{x}) \leq 0,\ \forall \boldsymbol{x}^\circ \in \boldsymbol{A}^{-1}\mathcal{C}\} \\ &= \boldsymbol{A}^{-\mathrm{T}}\,\mathcal{N}_{A^{-1}\mathcal{C}}(\boldsymbol{A}^{-1}\boldsymbol{x}).\end{aligned} \tag{22}$$

The proximal point function to the convex set $\mathcal{C}$ in a norm $\|.\|_R$ can be expressed with the proximal point function to the set $\boldsymbol{A}^{-1}\mathcal{C}$ in the norm $\|.\|_{A^{\mathrm{T}}RA}$

$$\mathrm{prox}_{\mathcal{C}}^{R}(\boldsymbol{x}) = \boldsymbol{A}\,\mathrm{prox}_{A^{-1}\mathcal{C}}^{A^{\mathrm{T}}RA}(\boldsymbol{A}^{-1}\boldsymbol{x}). \tag{23}$$

This equation can be verified using the definition of the proximal point function (4)

$$\begin{aligned}\mathrm{prox}_{\mathcal{C}}^{R}(\boldsymbol{x}) &= \operatorname*{argmin}_{\boldsymbol{x}^* \in \mathcal{C}} \|\boldsymbol{x} - \boldsymbol{x}^*\|_R \\ &= \{\boldsymbol{x}^* \mid \|\boldsymbol{x} - \boldsymbol{x}^*\|_R \leq \|\boldsymbol{x} - \boldsymbol{y}\|_R,\ \forall \boldsymbol{y} \in \mathcal{C},\ \boldsymbol{x}^* \in \mathcal{C}\} \\ &= \{\boldsymbol{A}\boldsymbol{x}^\circ \mid \|\boldsymbol{x} - \boldsymbol{A}\boldsymbol{x}^\circ\|_R \leq \|\boldsymbol{x} - \boldsymbol{A}\boldsymbol{z}\|_R,\ \forall \boldsymbol{A}\boldsymbol{z} \in \mathcal{C},\ \boldsymbol{A}\boldsymbol{x}^\circ \in \mathcal{C}\} \\ &= \boldsymbol{A}\,\{\boldsymbol{x}^\circ \mid \|\boldsymbol{x} - \boldsymbol{A}\boldsymbol{x}^\circ\|_R \leq \|\boldsymbol{x} - \boldsymbol{A}\boldsymbol{z}\|_R,\ \forall \boldsymbol{z} \in \boldsymbol{A}^{-1}\mathcal{C},\ \boldsymbol{x}^\circ \in \boldsymbol{A}^{-1}\mathcal{C}\} \\ &= \boldsymbol{A}\operatorname*{argmin}_{\boldsymbol{x}^\circ \in A^{-1}\mathcal{C}} \|\boldsymbol{x} - \boldsymbol{A}\boldsymbol{x}^\circ\|_R \\ &= \boldsymbol{A}\operatorname*{argmin}_{\boldsymbol{x}^\circ \in A^{-1}\mathcal{C}} \|\boldsymbol{A}(\boldsymbol{A}^{-1}\boldsymbol{x} - \boldsymbol{x}^\circ)\|_R \\ &= \boldsymbol{A}\operatorname*{argmin}_{\boldsymbol{x}^\circ \in A^{-1}\mathcal{C}} \|\boldsymbol{A}^{-1}\boldsymbol{x} - \boldsymbol{x}^\circ\|_{A^{\mathrm{T}}RA} \\ &= \boldsymbol{A}\,\mathrm{prox}_{A^{-1}\mathcal{C}}^{A^{\mathrm{T}}RA}(\boldsymbol{A}^{-1}\boldsymbol{x}).\end{aligned} \tag{24}$$

A normal cone inclusion $\boldsymbol{y} \in \mathcal{N}_{\mathcal{C}}(\boldsymbol{x})$ can be transformed into a normal cone inclusion on the inverse mapped set $\boldsymbol{A}^{-1}\mathcal{C}$ using (20),

$$\boldsymbol{y} \in \mathcal{N}_{\mathcal{C}}(\boldsymbol{x}) \quad \Leftrightarrow \quad \boldsymbol{A}^{\mathrm{T}}\boldsymbol{y} \in \mathcal{N}_{A^{-1}\mathcal{C}}(\boldsymbol{A}^{-1}\boldsymbol{x}). \tag{25}$$

This can be used to transform a normal cone inclusion on an elliptical set to a normal cone inclusion on a circular set as illustrated in Figure 1. Now, instead of directly rewriting the normal cone inclusion on $\mathcal{C}$ as a proximal point equation (cf. section 2),

$$\boldsymbol{y} \in \mathcal{N}_{\mathcal{C}}(\boldsymbol{x}) \quad \Leftrightarrow \quad \boldsymbol{x} = \mathrm{prox}_{\mathcal{C}}^{R}(\boldsymbol{x} + \boldsymbol{R}^{-1}\boldsymbol{y}), \tag{26}$$

the normal cone inclusion using the inverse mapped set $\boldsymbol{A}^{-1}\mathcal{C}$ can be rewritten. To achieve this, the right hand side of (25) is transformed into a proximal point equation by using the equivalence (26) which yields

$$\boldsymbol{A}^{\mathrm{T}}\boldsymbol{y} \in \mathcal{N}_{A^{-1}\mathcal{C}}(\boldsymbol{A}^{-1}\boldsymbol{x}) \quad \Leftrightarrow \quad \boldsymbol{A}^{-1}\boldsymbol{x} = \mathrm{prox}_{A^{-1}\mathcal{C}}^{\hat{R}}(\boldsymbol{A}^{-1}\boldsymbol{x} + \hat{\boldsymbol{R}}^{-1}\boldsymbol{A}^{\mathrm{T}}\boldsymbol{y}). \tag{27}$$

Here again the matrix $\hat{\boldsymbol{R}}$ can be chosen freely as long as it is symmetric and positive definite. If the right hand side of (26) is transformed to the inverse mapped set $\boldsymbol{A}^{-1}\mathcal{C}$ by using (23), one obtains the equation

$$\boldsymbol{x} = \boldsymbol{A}\,\mathrm{prox}_{A^{-1}\mathcal{C}}^{A^{\mathrm{T}}RA}(\boldsymbol{A}^{-1}\boldsymbol{x} + \boldsymbol{A}^{-1}\boldsymbol{R}^{-1}\boldsymbol{y}). \tag{28}$$

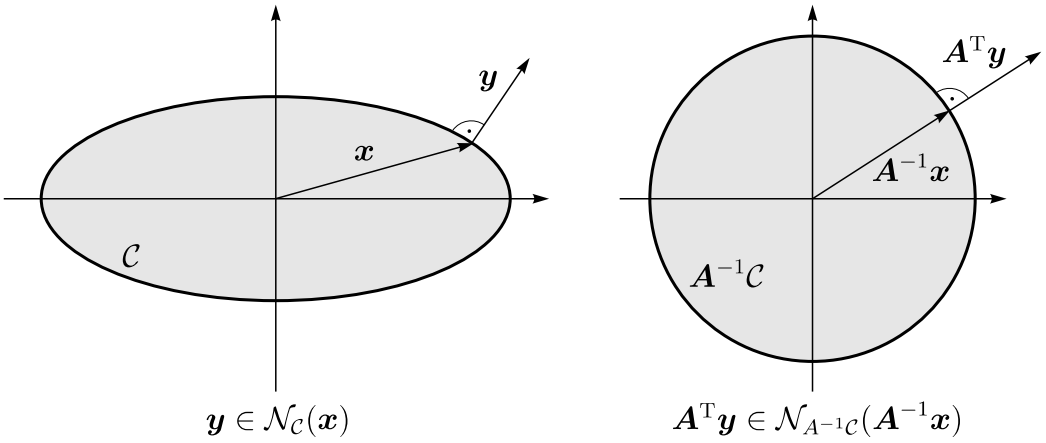

Figure 1: Transformation of the normal cone inclusion.

With the special choice

$$\boldsymbol{R} = \boldsymbol{A}^{-\mathrm{T}} \hat{\boldsymbol{R}}\, \boldsymbol{A}^{-1}, \tag{29}$$

equation (28) yields exactly the right hand side of (27). This means that we can transform the original normal cone inclusion $\boldsymbol{y} \in \mathcal{N}_{\mathcal{C}}(\boldsymbol{x})$ either to a normal cone inclusion on the inverse mapped set $\boldsymbol{A}^{-1}\mathcal{C}$ and then rewrite it as proximal point equation, or rewrite it directly into an equation and transform then the obtained proximal point problem to the set $\boldsymbol{A}^{-1}\mathcal{C}$. This can be illustrated as:

$$\begin{aligned} &\boldsymbol{y} \in \mathcal{N}_{\mathcal{C}}(\boldsymbol{x}) && \Leftrightarrow \quad \boldsymbol{A}^{\mathrm{T}}\boldsymbol{y} \in \mathcal{N}_{A^{-1}\mathcal{C}}(\boldsymbol{A}^{-1}\boldsymbol{x}) \\ &\quad \Updownarrow && \qquad\quad \Updownarrow \\ &\boldsymbol{x} = \operatorname{prox}^{R}_{\mathcal{C}}(\boldsymbol{x} + \boldsymbol{R}^{-1}\boldsymbol{y}) && \Leftrightarrow \quad \boldsymbol{A}^{-1}\boldsymbol{x} = \operatorname{prox}^{\hat{R}}_{A^{-1}\mathcal{C}}(\boldsymbol{A}^{-1}\boldsymbol{x} + \hat{\boldsymbol{R}}^{-1}\boldsymbol{A}^{\mathrm{T}}\boldsymbol{y}). \end{aligned} \tag{30}$$

It has to be noted that the constraint (29) on $\boldsymbol{R}$ and $\hat{\boldsymbol{R}}$ is only required for the identity

$$\operatorname{prox}^{R}_{\mathcal{C}}(\boldsymbol{x} + \boldsymbol{R}^{-1}\boldsymbol{y}) = \boldsymbol{A}\operatorname{prox}^{\hat{R}}_{A^{-1}\mathcal{C}}(\boldsymbol{A}^{-1}\boldsymbol{x} + \hat{\boldsymbol{R}}^{-1}\boldsymbol{A}^{\mathrm{T}}\boldsymbol{y}), \tag{31}$$

where just a general proximal point problem is transformed without exploiting the special structure of the normal cone inclusion (27). The symmetric and positive definite matrices $\boldsymbol{R}$ and $\hat{\boldsymbol{R}}$ can be chosen freely in (30), because the struture of the normal cone inclusion is available there. By renaming the transformed vectors and sets

$$\boldsymbol{x} = \boldsymbol{A}\hat{\boldsymbol{x}}, \quad \mathcal{C} = \boldsymbol{A}\hat{\mathcal{C}}, \quad \hat{\boldsymbol{y}} = \boldsymbol{A}^{\mathrm{T}}\boldsymbol{y} \tag{32}$$

one can recognize that the structure of the problem remains exactly the same for both the formulations based on $\mathcal{C}$ and those based on the inverse mapped set $\boldsymbol{A}^{-1}\mathcal{C}$.

$$\begin{aligned} &\boldsymbol{y} \in \mathcal{N}_{\mathcal{C}}(\boldsymbol{x}) && \Leftrightarrow \quad \hat{\boldsymbol{y}} \in \mathcal{N}_{\hat{\mathcal{C}}}(\hat{\boldsymbol{x}}) \\ &\quad \Updownarrow && \qquad\quad \Updownarrow \\ &\boldsymbol{x} = \operatorname{prox}^{R}_{\mathcal{C}}(\boldsymbol{x} + \boldsymbol{R}^{-1}\boldsymbol{y}) && \Leftrightarrow \quad \hat{\boldsymbol{x}} = \operatorname{prox}^{\hat{R}}_{\hat{\mathcal{C}}}(\hat{\boldsymbol{x}} + \hat{\boldsymbol{R}}^{-1}\hat{\boldsymbol{y}}) \end{aligned} \tag{33}$$

5 EFFICIENT PROXIMAL POINT FORMULATION

In section 3, a system of normal cone inclusions has been obtained after the discretisation of the equations of motion of a non-smooth mechanical system

$$\boldsymbol{\xi}_i \in \mathcal{N}_{\mathcal{D}_i}(-\boldsymbol{\Lambda}_i), \quad \boldsymbol{\xi}_i = \sum_j \boldsymbol{G}_{ij}\boldsymbol{\Lambda}_j + \boldsymbol{c}_i, \tag{34}$$

which have to be solved for every integration step. In order to solve these inclusions numerically, they are usually rewritten as proximal point equations

$$-\boldsymbol{\Lambda}_i = \operatorname{prox}_{\mathcal{D}_i}(-\boldsymbol{\Lambda}_i + r_i\boldsymbol{\xi}_i), \quad \boldsymbol{\xi}_i = \sum_j \boldsymbol{G}_{ij}\boldsymbol{\Lambda}_j + \boldsymbol{c}_i \tag{35}$$

where the matrix $\boldsymbol{R}_i$ has been chosen as $\frac{1}{r_i}\boldsymbol{I}$ to keep the proximal point function $\operatorname{prox}_{\mathcal{D}_i}$ in the Euclidian norm. After eliminating $\boldsymbol{\xi}_i$ one obtains the equations

$$-\boldsymbol{\Lambda}_i = \operatorname{prox}_{\mathcal{D}_i}(-\boldsymbol{\Lambda}_i + r_i \sum_j \boldsymbol{G}_{ij}\boldsymbol{\Lambda}_j + r_i\, \boldsymbol{c}_i), \tag{36}$$

which can then be iterated for a fixpoint with a projected Jacobi scheme

$$\boldsymbol{\Lambda}_i^{\nu+1} = -\operatorname{prox}_{\mathcal{D}_i}(-\boldsymbol{\Lambda}_i^{\nu} + r_i \sum_j \boldsymbol{G}_{ij}\boldsymbol{\Lambda}_j^{\nu} + r_i\, \boldsymbol{c}_i). \tag{37}$$

For each iteration the proximal point function $\operatorname{prox}_{\mathcal{D}_i}$ has to be evaluated. In general, calculating the nearest point in a set involves the solution of an implicit function. This is not very efficient and it has to be done for every step of the fixpoint iteration. The first idea is to transform the proximal point functions in the equations (36) from the sets $\mathcal{D}_i$ to simpler sets $\boldsymbol{A}_i^{-1}\mathcal{D}_i$ with respect to proximal points. If the set $\mathcal{D}_i$ is an ellipse, then the matrix $\boldsymbol{A}_i$ can be chosen such that $\boldsymbol{A}_i^{-1}\mathcal{D}_i$ is a circular disc. The proximal point function to a circular disc in the Euclidian norm can be implemented very efficiently. Unfortunately, the transformation of an equation (36) with the help of (23) yields the equation

$$-\boldsymbol{\Lambda}_i = \boldsymbol{A}_i \operatorname{prox}^{A_i^{\mathrm{T}}A_i}_{A_i^{-1}\mathcal{D}_i}(-\boldsymbol{A}_i^{-1}\boldsymbol{\Lambda}_i + r_i\, \boldsymbol{A}_i^{-1} \sum_j \boldsymbol{G}_{ij}\boldsymbol{\Lambda}_j + r_i\, \boldsymbol{A}_i^{-1}\boldsymbol{c}_i) \tag{38}$$

which contains a proximal point function to the simplified set $\boldsymbol{A}_i^{-1}\mathcal{D}_i$ but in the $\|.\|_{A_i^{\mathrm{T}}A_i}$ norm. Evaluating the proximal point function to the set $\boldsymbol{A}_i^{-1}\mathcal{D}_i$ in the norm $\|.\|_{A_i^{\mathrm{T}}A_i}$ is not more efficient than evaluating the original proximal point function to the set $\mathcal{D}_i$ in the Euclidian norm. The problem here is, that we try to transform a general proximal point problem without using the fact that it originates from a normal cone inclusion. The special structure of the problem can be exploited by applying the transformation directly to the normal cone inclusion and then reformulating the transformed inclusion as a proximal point equation as outlined in the last section. This means that relationship (30) is applied to the inclusion (34), yielding

$$\boldsymbol{\xi}_i \in \mathcal{N}_{\mathcal{D}_i}(-\boldsymbol{\Lambda}_i) \quad \Leftrightarrow \quad -\boldsymbol{A}_i^{-1}\boldsymbol{\Lambda}_i = \operatorname{prox}^{\hat{R}_i}_{A_i^{-1}\mathcal{D}_i}(-\boldsymbol{A}_i^{-1}\boldsymbol{\Lambda}_i + \hat{\boldsymbol{R}}_i^{-1}\boldsymbol{A}_i^{\mathrm{T}}\boldsymbol{\xi}_i). \tag{39}$$

After choosing $\hat{\boldsymbol{R}}_i$ as $\frac{1}{\hat{r}_i}\boldsymbol{I}$ one obtains the equation

$$-\boldsymbol{\Lambda}_i = \boldsymbol{A}_i \operatorname{prox}_{A_i^{-1}\mathcal{D}_i}(-\boldsymbol{A}_i^{-1}\boldsymbol{\Lambda}_i + \hat{r}_i\, \boldsymbol{A}_i^{\mathrm{T}} \sum_j \boldsymbol{G}_{ij}\boldsymbol{\Lambda}_j + \hat{r}_i\, \boldsymbol{A}_i^{\mathrm{T}}\boldsymbol{c}_i) \tag{40}$$

which now uses a proximal point function in the Euclidian norm and to the inverse mapped set $\boldsymbol{A}_i^{-1}\mathcal{D}_i$. Before iterating this equation for a fixpoint it is useful to introduce the definitions

$$\hat{\boldsymbol{\xi}}_i := \boldsymbol{A}_i^{\mathrm{T}}\boldsymbol{\xi}_i, \quad \hat{\boldsymbol{\Lambda}}_i := \boldsymbol{A}_i^{-1}\boldsymbol{\Lambda}_i, \quad \hat{\boldsymbol{G}}_{ij} := \boldsymbol{A}_i^{\mathrm{T}}\boldsymbol{G}_{ij}\boldsymbol{A}_j \quad \hat{\boldsymbol{c}}_i := \boldsymbol{A}_i^{\mathrm{T}}\boldsymbol{c}_i, \tag{41}$$

simplifying equation (40) to

$$-\hat{\boldsymbol{\Lambda}}_i = \mathrm{prox}_{A_i^{-1}\mathcal{D}_i}(-\hat{\boldsymbol{\Lambda}}_i + \hat{r}_i \sum_j \hat{\boldsymbol{G}}_{ij}\hat{\boldsymbol{\Lambda}}_j + \hat{r}_i\, \hat{\boldsymbol{c}}_i) \tag{42}$$

which has again the same structure as equation (36). The projected Jacobi fixpoint scheme then becomes

$$\hat{\boldsymbol{\Lambda}}_i^{\nu+1} = -\mathrm{prox}_{A_i^{-1}\mathcal{D}_i}(-\hat{\boldsymbol{\Lambda}}_i^{\nu} + \hat{r}_i \sum_j \hat{\boldsymbol{G}}_{ij}\hat{\boldsymbol{\Lambda}}_j^{\nu} + \hat{r}_i\, \hat{\boldsymbol{c}}_i), \quad \hat{r}_i = \frac{\alpha}{\max\limits_k(\hat{\boldsymbol{G}}_{iikk})}, \tag{43}$$

where $\hat{\boldsymbol{G}}_{iikk}$ denotes the k-th diagonal element of the matrix $\hat{\boldsymbol{G}}_{ii}$. The parameter $\hat{r}_i$ is chosen as the smallest inverse diagonal term $1/\max_k(\hat{\boldsymbol{G}}_{iikk})$ of the matrix $\hat{\boldsymbol{G}}_{ii}$ multiplied by an optional relaxation factor $0 < \alpha < 2$. In the non-projecting case, that means if the argument of the proximal point function in (43) is in the inverse mapped set,

$$-\hat{\boldsymbol{\Lambda}}_i^{\nu} + \hat{r}_i \sum_j \hat{\boldsymbol{G}}_{ij}\hat{\boldsymbol{\Lambda}}_j^{\nu} + \hat{r}_i\, \hat{\boldsymbol{c}}_i \in \boldsymbol{A}_i^{-1}\mathcal{D}_i, \tag{44}$$

the iteration reduces to the Jacobi like fixpoint iteration

$$\hat{\boldsymbol{\Lambda}}_i^{\nu+1} = \hat{\boldsymbol{\Lambda}}_i^{\nu} - \frac{\alpha}{\max\limits_k(\hat{\boldsymbol{G}}_{iikk})}\Big(\sum_j \hat{\boldsymbol{G}}_{ij}\hat{\boldsymbol{\Lambda}}_j^{\nu} + \hat{\boldsymbol{c}}_i\Big). \tag{45}$$

In cases where the diagonal elements of the matrix $\hat{\boldsymbol{G}}_{ii}$ are of different order of magnitude the convergence of the iteration can be slow compared to the original Jacobi iteration. In such a badly scaled case, one can replace the scheme (43) with

$$\begin{aligned}
\hat{\boldsymbol{\Lambda}}_i^{\nu+1} &= \hat{\boldsymbol{\Lambda}}_i^{\nu} - \boldsymbol{Q}_i^{\nu}\Big(\mathrm{prox}_{A_i^{-1}\mathcal{D}_i}(-\hat{\boldsymbol{\Lambda}}_i^{\nu} + \hat{r}_i \sum_j \hat{\boldsymbol{G}}_{ij}\hat{\boldsymbol{\Lambda}}_j^{\nu} + \hat{r}_i\, \hat{\boldsymbol{c}}_i) + \hat{\boldsymbol{\Lambda}}_i^{\nu}\Big) \\
\boldsymbol{Q}_i^{\nu} &= \begin{cases} \mathrm{diag}\,\dfrac{\alpha}{\hat{r}_i\hat{\boldsymbol{G}}_{iikk}}, & -\hat{\boldsymbol{\Lambda}}_i^{\nu} + \hat{r}_i \sum_j \hat{\boldsymbol{G}}_{ij}\hat{\boldsymbol{\Lambda}}_j^{\nu} + \hat{r}_i\, \hat{\boldsymbol{c}}_i \in A_i^{-1}\mathcal{D}_i \\ \boldsymbol{I}, & \text{else} \end{cases} \\
\hat{r}_i &= \frac{\alpha}{\max\limits_k(\hat{\boldsymbol{G}}_{iikk})},
\end{aligned} \tag{46}$$

which recovers the performance of the original Jacobi iteration in the non-projecting case while keeping the properties in projecting situations. This iteration scheme has the same fixpoint as (43) since the matrix $\boldsymbol{Q}_i$ is regular. After a solution for $\hat{\boldsymbol{\Lambda}}_i$ has been found, the solution for the original discrete percussion $\boldsymbol{\Lambda}_i$ can be calculated as

$$\boldsymbol{\Lambda}_i = \boldsymbol{A}_i\hat{\boldsymbol{\Lambda}}_i. \tag{47}$$

6 COULOMB-CONTENSOU FRICTION

The set-valued force law for Coulomb-Contensou friction can be used to model a contact with Coulomb friction and drilling friction torque [4]. The drilling friction force is the result of an area with distributed Coulomb friction. The force law is formulated by using two translational scalar friction forces λ_{T_1}, λ_{T_2} and a scalar friction moment λ_τ as shown in Figure 2. Each

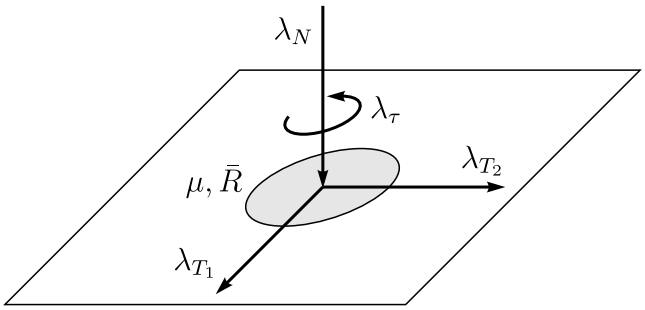

Figure 2: Coulomb-Contensou friction forces.

of the scalar forces λ_{T_1}, λ_{T_2} and λ_τ has it corresponding relative velocity γ_{T_1}, γ_{T_2} and γ_τ. The translational forces and velocities are grouped into vectors to simplify the notation,

$$\boldsymbol{\lambda}_T := \begin{pmatrix} \lambda_{T_1} \\ \lambda_{T_2} \end{pmatrix}, \quad \boldsymbol{\gamma}_T := \begin{pmatrix} \gamma_{T_1} \\ \gamma_{T_2} \end{pmatrix}. \tag{48}$$

The scalar force λ_N is provided by the associated normal force law. As parameters, the Coulomb friction coefficient μ and the average friction radius $\bar{R}$ are used. For pure translational Coulomb friction, this results in a maximal friction force of $\mu\lambda_N$, while pure rotational friction gives a maximum friction moment of $\bar{R}\mu\lambda_N$. In general, the three friction forces and relative velocities are not independent, especially the drilling friction interacts with the translational friction. In [4] a force law of the form

$$\begin{pmatrix} \boldsymbol{\gamma}_T \\ \gamma_\tau \end{pmatrix} \in \mathcal{N}_{\mathcal{B}_F}\Big(- \begin{pmatrix} \boldsymbol{\lambda}_T \\ \lambda_\tau \end{pmatrix}\Big) \tag{49}$$

has been derived for a contact with a circular contact area on which a Coulomb friction interaction is formulated in each point and the normal force λ_N is parabolically distributed (Hertz). A more general approach to the reduction of distributed set-valued force laws and their application to Coulomb-Contensou friction can be found in [2]. In the case of parabolic normal force distribution, the average friction radius $\bar{R}$ is

$$\bar{R} = \frac{3\pi}{16} R \approx 0.589R, \tag{50}$$

where R is the radius of the assumed circular contact area. The functions

$$b_T(u) := \begin{cases} \dfrac{3\pi\mu\lambda_N}{32}(-u^3 + 4u), & u \leq 1 \\ \dfrac{3\mu\lambda_N}{16}\left((-u^3 + 4u)\arcsin\left(\dfrac{1}{u}\right) + \dfrac{1}{u}(u^2+2)\sqrt{u^2-1}\right), & u > 1 \end{cases} \tag{51}$$

and

$$b_\tau(u) := \begin{cases} \dfrac{\bar{R}\mu\lambda_N}{8}(3u^4 - 8u^2 + 8), & u \leq 1 \\ \dfrac{\bar{R}\mu\lambda_N}{4\pi}\left((3u^4 - 8u^2 + 8)\arcsin\left(\dfrac{1}{u}\right) + (-3u^2+6)\sqrt{u^2-1}\right), & u > 1 \end{cases} \tag{52}$$

give a parametric description of the boundary of the set $\mathcal{B}_F$. The set $\mathcal{B}_F$ is then described by the implicit formulation

$$\mathcal{B}_F := \left\{ \begin{pmatrix} \boldsymbol{\lambda}_T \\ \lambda_\tau \end{pmatrix} \mid \|\boldsymbol{\lambda}_T\| \leq b_T(u),\ |\lambda_\tau| \leq b_\tau(u),\ u \in [0,\infty) \right\}. \tag{53}$$

The set is rotationally symmetric around the λ_τ-axis and has the cross-section shown in Figure 3. The normal cone inclusion (49) together with the set $\mathcal{B}_F$ gives the exact condensed force law for a contact with perfectly circular contact area, parabolic Hertz normal pressure distribution and a distributed Coulomb friction law. Unfortunately, calculating the proximal point to this set in the Euclidian norm is complicated and time-consuming. The simplest approximation of the

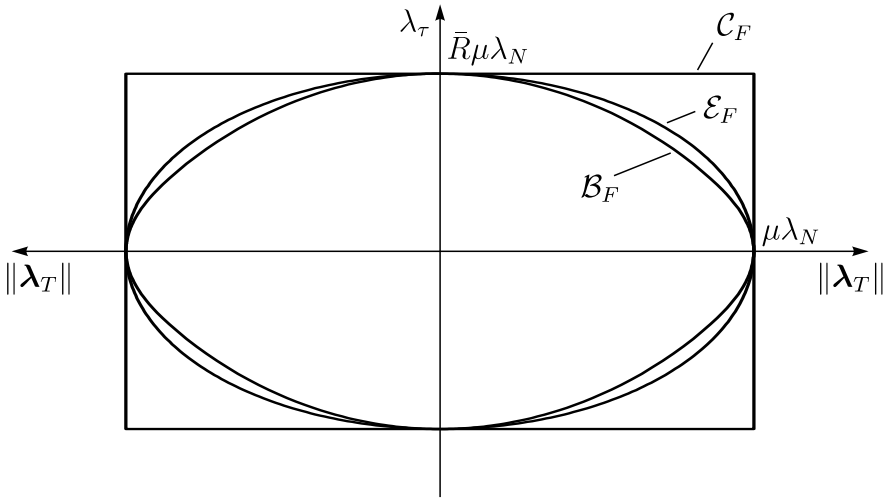

Figure 3: Approximations of Coulomb-Contensou friction.

set $\mathcal{B}_F$ would be a cylindrical set $\mathcal{C}_F$ with the λ_τ-axis as axis of symmetry, a radius equal to $\mu\lambda_N$ and a height of $2\bar{R}\mu\lambda_N$

$$\mathcal{C}_F := \left\{ \begin{pmatrix} \boldsymbol{\lambda}_T \\ \lambda_\tau \end{pmatrix} \mid \|\boldsymbol{\lambda}_T\| \leq \mu\lambda_N,\ |\lambda_\tau| \leq \bar{R}\mu\lambda_N \right\}. \tag{54}$$

For the set $\mathcal{C}_F$, the proximal point function $\mathrm{prox}_{\mathcal{C}_F}$ is very simple and the projection can even be decoupled in λ_τ and $\boldsymbol{\lambda}_T$ direction. But exactly this decoupling is not desired, because the interaction between drilling friction and the translational friction is an important property of the model. A better approximation is an ellipsoidal set $\mathcal{E}_F$ with one semi-axis of $\bar{R}\mu\lambda_N$ and the other two of $\mu\lambda_N$ (cf. cross section in Figure 3),

$$\mathcal{E}_F := \left\{ \begin{pmatrix} \boldsymbol{\lambda}_T \\ \lambda_\tau \end{pmatrix} \mid \left(\frac{\|\boldsymbol{\lambda}_T\|}{\mu\lambda_N} \right)^2 + \left(\frac{\lambda_\tau}{\bar{R}\mu\lambda_N} \right)^2 \leq 1 \right\}. \tag{55}$$

Further approximations for Coulomb-Contensou friction and a comparison with experimental results can be found in [3]. The elliptical set (55) can be transformed to a sphere $\mathcal{S}_F$ with radius $\mu\lambda_N$ by introducing the matrix

$$\boldsymbol{A} = \begin{pmatrix} 1 & 0 & 0 \\ 0 & 1 & 0 \\ 0 & 0 & \bar{R} \end{pmatrix}, \tag{56}$$

and applying the inverse mapping

$$\boldsymbol{A}^{-1}\mathcal{E}_F = \mathcal{S}_F. \tag{57}$$

The resulting set

$$\mathcal{S}_F := \left\{ \begin{pmatrix} \boldsymbol{\lambda}_T \\ \lambda_\tau \end{pmatrix} \mid \|\boldsymbol{\lambda}_T\|^2 + \lambda_\tau^2 \leq \mu^2\lambda_N^2 \right\} \tag{58}$$

allows then for an explicit closed form describtion of the proximal point function

$$\operatorname{prox}_{\mathcal{S}_F}\left(\begin{pmatrix}\boldsymbol{\lambda}_T\\ \lambda_\tau\end{pmatrix}\right)=\begin{cases}\begin{pmatrix}\boldsymbol{\lambda}_T\\ \lambda_\tau\end{pmatrix}, & \|\boldsymbol{\lambda}_T\|^2+\lambda_\tau^2\leq\mu^2\lambda_N^2\\ \dfrac{\mu\lambda_N}{\sqrt{\|\boldsymbol{\lambda}_T\|^2+\lambda_\tau^2}}\begin{pmatrix}\boldsymbol{\lambda}_T\\ \lambda_\tau\end{pmatrix}, & \|\boldsymbol{\lambda}_T\|^2+\lambda_\tau^2>\mu^2\lambda_N^2\end{cases} \tag{59}$$

which can be evaluated very efficiently.

In the following, the simplified Coulomb-Contensou force law, based on $\mathcal{E}_F$ is used in a model of the Tippe-Top and is compared to results obtained with the set $\mathcal{B}_F$. The Tippe-Top is modeled as rigid body with two contacts and Coulomb-Contensou friction using the set $\mathcal{E}_F$ or $\mathcal{B}_F$. The geometric, mass and contact parameters as well as initial conditions are identical to those published in [4]. The orientation is parametrized with quaternions. For the numerical solution, the time stepping scheme described in section 3 with the fixpoint iteration (46) is used. In the case of the force law using the ellipsoidal set $\mathcal{E}_F$, the fixpoint iteration has been implemented in both ways, one using a spherical set $\mathcal{S}_F$ with the proximal point function $\operatorname{prox}_{\mathcal{S}_F}$ and the other based on the original set. In Figure 4, the inclination angle vs. time is shown for the Tippe-Top with friction laws based on the set $\mathcal{E}_F$ and $\mathcal{B}_F$. Of course, the results start to deviate with time because the system is very sensitive, but still the overall behaviour is preserved very well. A MATLAB® implementation results in a fixpoint iteration for the set $\mathcal{S}_F$ which is about

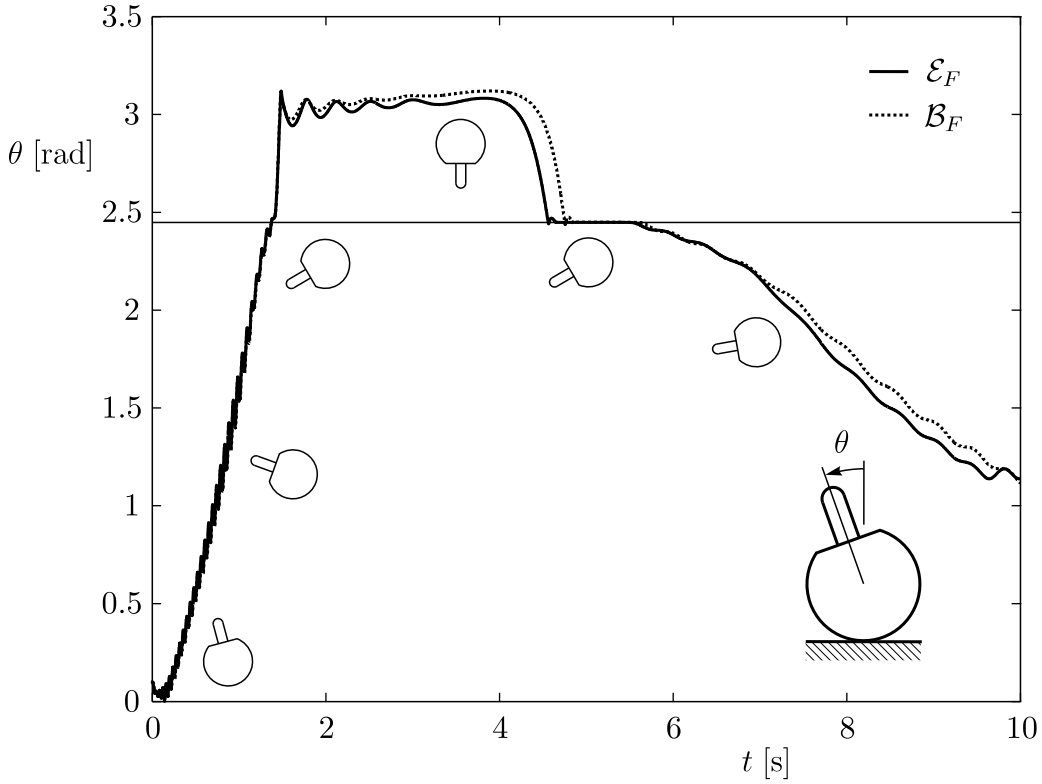

Figure 4: Inclination of the Tippe-Top.

10.5 times faster than with $\mathcal{B}_F$. Compared to the set $\mathcal{E}_F$, the fixpoint iteration for the set $\mathcal{S}_F$ is about 2.7 times faster. It has to be noted here, that the solution obtained with the set $\mathcal{B}_F$ is

only more correct with respect to the assumptions made about the contact area and the friction interaction. In general, the geometry of the contact area, the distribution of the normal force in the contact area and the properties of the friction interaction are subject to large uncertainties. In this situation, the level of model-detail of the ellipsoidal set can be more appropriate.

7 CONCLUSIONS

An efficient method for the solution of normal cone inclusions on elliptical (or ellipsoidal) sets was presented in this paper. For approximated Coulomb-Contensou friction, the method leads to a simpler and faster implementation. A modified iterative projection method for the solution of multi-dimensional set-valued force laws was proposed. This method helps to recover the iteration performance for badly scaled problems in the non-projecting case. The presented techniques have been tested successfully on a numerical simulation of the Tippe-Top.

REFERENCES

[1] Ch. Glocker, Simulation von harten Kontakten mit Reibung: Eine iterative Projektionsmethode. *VDI-Berichte Nr. 1968: Schwingungen in Antrieben 2006 Tagung, Fulda*, 19-44, VDI-Verlag, Düsseldorf, 2006.

[2] Ch. Glocker, Reduction Techniques for Distributed Set-Valued Force Laws. In *Proceedings of the 2nd International Conference on Nonsmooth/Nonconvex Mechanics with Applications in Engineering (Ed. C. C. Baniotopoulos), Thessaloniki, Greece, July 2006*, 173-180, Editions Ziti, Thessaloniki, 2006.

[3] R. D. Howe, M. R. Cutkosky, Practical Force-Motion Models for Sliding Manipulation. *The International Journal of Robotics Research*, **15**(6), 557-572, 1996.

[4] R. I. Leine, Ch. Glocker, A Set-valued Force Law for Spatial Coulomb-Contensou Friction. *European Journal of Mechanics A/Solids*, **22**, 193-216, 2003.

[5] J. J. Moreau, Unilateral contact and dry friction in finite freedom dynamics. In *Non-Smooth Mechanics and Applications*, J. J. Moreau, P. D. Panagiotopoulos, Eds., vol. 302 of *CISM Courses and Lectures*, 1-82, Springer, Wien, 1988.

[6] C. Studer, R. I. Leine, Ch. Glocker, Step size adjustment and extrapolation for time-stepping schemes in non-smooth dynamics. *Int. J. Numer. Meth. Engng*, **76**, 1747-1781, 2008.